Int. J. Electrochem. Sci., 13 **(2018)** 5824 – 5831, doi: 10.20964/2018.06.42

International Journal of
ELECTROCHEMICAL
SCIENCE
www.electrochemsci.org

Enhancement of Cycling Stability of $LiMnPO_4$ at Elevated Temperature by Fe-Mg co-Substitution

Chenglin Hu, Bin Wang, Huihua Yi[*], *Juping Zhang, Yanhui Hu, Jiahao Li*

Institute for Quantum Materials/School of Materials Science and Engineering/Hubei Key Laboratory of Mine Environmental Pollution Control & Remediation, Hubei Polytechnic University, Huangshi 435003, China
[*]E-mail: yihuihua@126.com

Received: 28 January 2018 / *Accepted:* 10 April 2018 / *Published:* 10 May 2018

Olivine-type $LiMnPO_4$ has been extensively investigated as a promising cathode material for the next-generation high performance Li-ion batteries due to its high working voltage (4.1 V vs Li^+/Li) and high theoretical specific capacity (170 mAh g^{-1}). However, poor cycling performance at elevated temperature hinders its practical application. Here carbon coating and Fe-Mg co-substitution of $LiMnPO_4$ is attempted by a facile solid-state process. To substitute the smaller Fe^{2+} ions and Mg^{2+} ions for the larger Mn^{2+} ions strengthens the Mn-O bond, which makes the structure of $LiMnPO_4$ more stable. Hence, Mn dissolution in the electrolyte is retrained. The obtained $LiMn_{0.9}Fe_{0.09}Mg_{0.01}PO_4/C$ material presents a high discharge capacity (160 mAh g^{-1} at 0.1 C) and excellent cycling performance at elevated temperature. Even at a high rate of 1 C, it delivers a capacity of about 135 mAh g^{-1} at 50 °C without capacity fade after 120 cycles.

Keywords: Lithium-ion batteries; Lithium Manganese Phosphate; Mn dissolution; elevated temperature; co-substitution

1. INTRODUCTION

Since the original work of Goodenough Group [1] was published in 1997, olivine-type compounds $LiMPO_4$ (M = Mn, Fe, Co, Ni) have been investigated extensively as promising cathode materials for lithium-ion batteries [2-12]. Among these compounds, $LiFePO_4$ has been successfully applied in commercial industry [13]. Inspired by the success of $LiFePO_4$, $LiMnPO_4$ has attracted considerable attention in recent years owing to its high Li^+ intercalation potential of 4.1 V versus Li^+/Li. Unfortunately, $LiMnPO_4$ material suffers from low electrochemical activity and poor cycling stability. The low electrochemical activity is attributed to the poor intrinsic electronic conductivity and sluggish Li^+ ion diffusion kinetics [14-16]. The poor cycling stability arises from Jahn-Teller

distortions in delithiated phase $MnPO_4$ and the disolution of Mn in electrolyte [17-19].

During the past two decades, significant efforts have been made to improve $LiMnPO_4$ material [5-12]. The electrochemical performance of this material was enhanced by conductive additive coating [19-22], particle size reduction [23-27] and cation doping or subsitution [28-33]. Nowadays, $LiMnPO_4$-based compounds can achieve nearly theoretical capacity and good high rate capability even at 10 C through optimized synthesis procedures [26-28]. However, capacity fading was still observed for $LiMnPO_4$ composites after full charge/discharge cycles [26,34], especially at elevated temperature [19,35-40]. The main reason is due to Mn ion dissolution in electrolyte and Jahn-Teller effect leading to the structure change like $LiMn_2O_4$ spinel [41,42]. There is very little report on improving the electrochemical performance of $LiMnPO_4$ at elevated temperature, which has been remaining as a challenge for its practical application.

In this work, we tried to prepare a carbon-coated and Fe-Mg co-substituted $LiMn_{0.9}Fe_{0.09}Mg_{0.01}PO_4/C$ by a simple solid-state method, and the primary results show that its electrochemical performance at 50 ^oC is markedly improved.

2. EXPERIMENTAL

Carbon coated $LiMnPO_4$ (LMP) and $LiMn_{0.9}Fe_{0.09}Mg_{0.01}PO_4$ (Fe-Mg) were synthesized by a simple solid-state reaction based on our previous reports [33,43]. Stoichiometric amounts of LiH_2PO_4, $MnC_4H_6O_4{\cdot}4H_2O$, $H_2C_2O_4{\cdot}2H_2O$, $FeC_2O_4{\cdot}2H_2O$ and $MgC_4H_6O_4{\cdot}4H_2O$ were mixed with 14 wt.% of sucrose by ball-milling for 6 h. The milled mixture was heated at 700 °C for 10 h under an Ar atmosphere. The residual carbon content in the final products is about 8 wt.% determined by VarioEL III elemental analyzer.

Cathode was made by mixing active material, conductive carbon black (Super P, Timcal) and polyvinylidene fluoride (PVDF, Atofina) in a weight ratio of 8:1:1. The electrodes were assembled into 2016 coin-type cells using Li metal foil as the counter electrode and reference electrode, Teklon separator (UH20140, Entek) and liquid electrolyte containing 1 M LiPF6 in a mixed solvent of EC/DMC/EMC by weight 1: 1: 1 (LB-315, Guotai-Huarong). These cells were charge at 0.1 C (1 C = 150 mA g^{-1}) to 4.6 V, and then discharged to 2.5 V with the same rate. Cyclic voltammetry (CV) curves were recorded at 0.2 mV s^{-1} from 2.0 to 4.8 V. Electrochemical impedance spectroscopy (EIS) was carried out in a frequency range from 0.1 Hz to 100 kHz with an AC signal of 5 mV. All electrochemical tests were performed at room temperature (RT)or at 50 °C in the oven. After 50 cycles, the half cells were disassembled and soaked in acetone for 24 h to detect the dissolution of Mn using inductively coupled plasma optical emission spectrometry (ICP, Hitachi P-4010).

3. RESULTS AND DISCUSSION

Figure 1 shows the XRD patterns of $LiMnPO_4/C$ and $LiMn_{0.9}Fe_{0.09}Mg_{0.01}PO_4/C$. Intense diffraction peaks are observed, which can be indentified as a single-phase olivine compound with

orthorhombic structure, Pnma space group. Partial Mn in $LiMnPO_4$ was substituted with Fe-Mg leading to a position shift of the diffraction peaks towards higher angles due to the ionic radius reduction (Mn^{2+}, 0.83 Å; Fe^{2+}, 0.78 Å; and Mg^{2+}, 0.72 Å) [44]. The refined lattice parameters were a = 6.1154 Å, b = 10.4665 Å, and c = 4.7467 Å for $LiMnPO_4$/C and a = 6.1002 Å, b = 10.4462 Å, and c = 4.7470 Å for $LiMn_{0.9}Fe_{0.09}Mg_{0.01}PO_4$/C. The calculated results also show a reduction of the unit cell volume from 303.82 to 302.49 $Å^3$ as 10% Mn was substituted with Fe-Mg. Substituting the smaller Fe^{2+} and Mg^{2+} for the larger Mn^{2+} shortens the Mn-O bond (inductive effect), increases the covalence of the Mn-O bond and raises the $Mn^{2+}/^{3+}$ redox energy [45]. It is advantageous in enhancing the stability of the olivine structure.

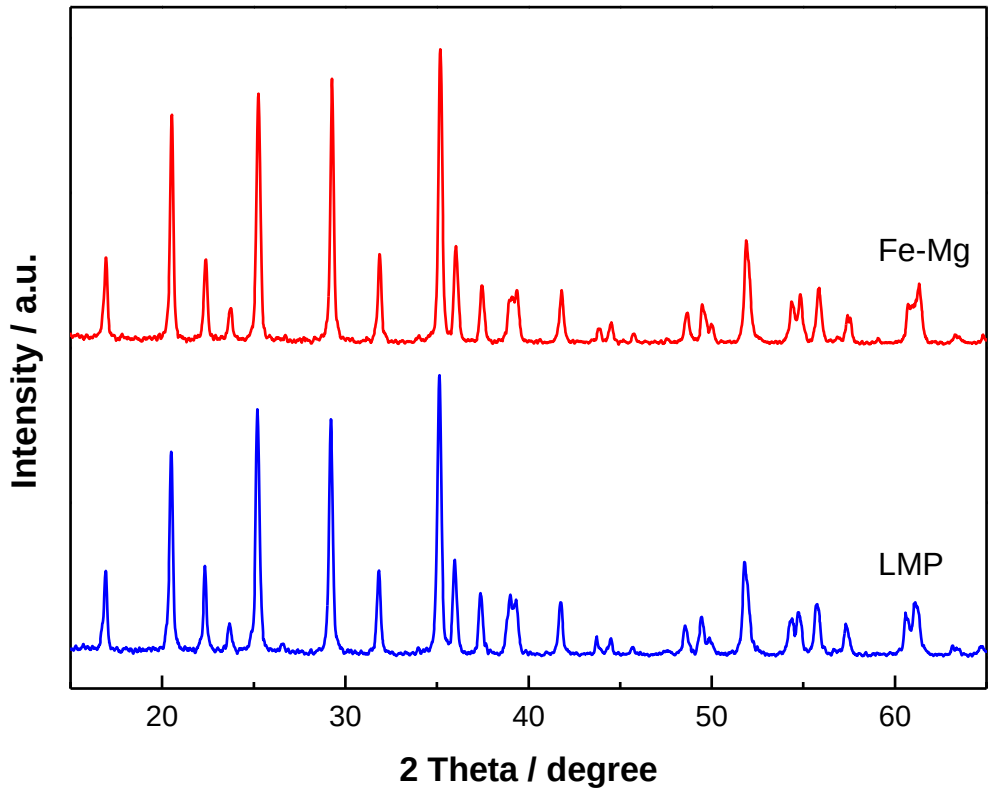

Figure 1. XRD patterns of $LiMnPO_4$/C (LMP) and $LiMn_{0.9}Fe_{0.09}Mg_{0.01}PO_4$/C (Fe-Mg).

Electrochemical behavior of the pristine and the Fe-Mg co-doped $LiMnPO_4$ was investigated by cyclic voltammetry at room temperature (RT) and at 50 °C, respectively. As shown in Figure 2, all samples present the anodic peaks and cathodic peaks of typical $LiMnPO_4$ as the cells were scanned 3 cycles from 2.0 to 4.8 V at 0.2 mV s^{-1}. At the first cycle, the broadening of anodic peaks suggest the formation of passivation layers of electrode surface for both samples tested at room temperature (Figure 2a&c), which become strong and sharp in the following two cycles. Sharp and symmetric redox peaks demonstrate high reversibility of the two samples at room temperature. However, at elevated temperature of 50 °C, the anodic peak including multi-oxidation peaks (Figure 2b) is attributed to the side reactions implying that the electrode of $LiMnPO_4$/C was faded upon cycling. At

the same condition, $LiMn_{0.9}Fe_{0.09}Mg_{0.01}PO_4/C$ exhibits good reversibility and the polarization is very weak (Figure 2d) due to the enhancement of electrochemical kinetics.

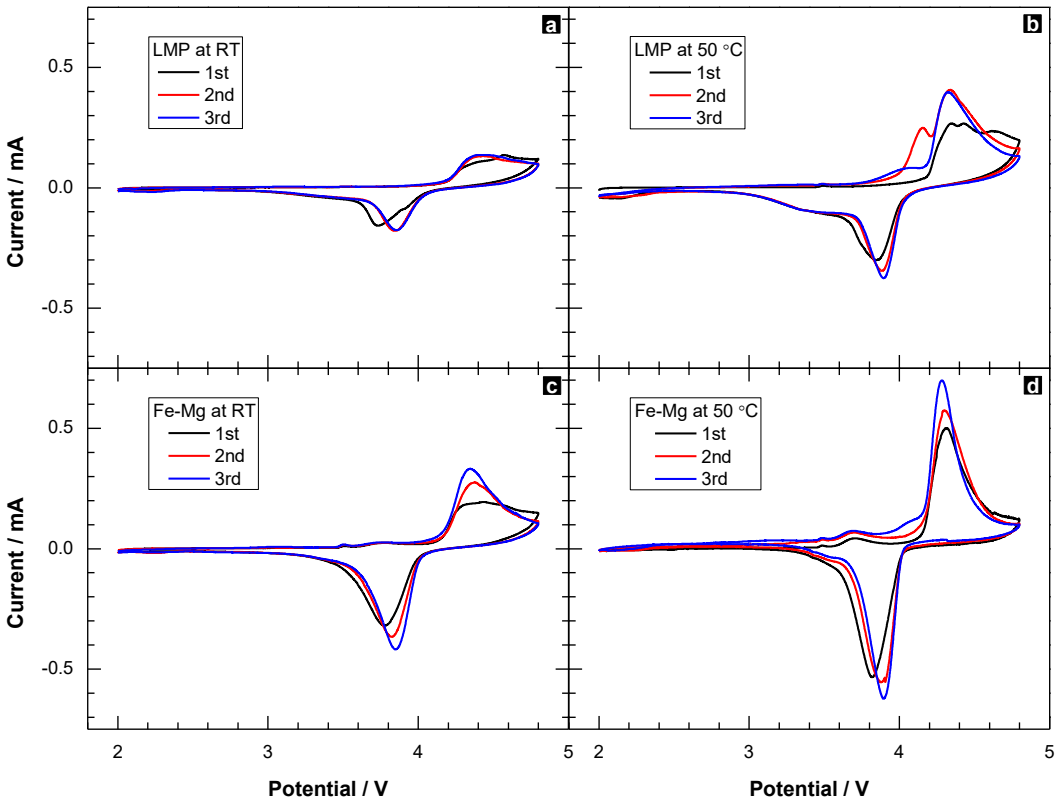

Figure 2. CV profiles of the cells at different temperatures with a scan rate of 0.2 mV s^{-1}: $LiMnPO_4/C$ (LMP) at (a) RT and (b) 50 °C; $LiMn_{0.9}Fe_{0.09}Mg_{0.01}PO_4/C$ (Fe-Mg) at (c) RT and (d) 50 °C.

To study the cycling performance of unsubstituted and Fe-Mg co-substituted $LiMnPO_4$ at elevated temperature, galvanostatic charge/discharge measurements were carried out at 50 °C between 4.6 and 2.5 V with 0.1 C. For comparison, both of the samples were also tested at room temperature. Figure 3a gives the charge/discharge curves of unsubstituted and Fe-Mg co-substituted $LiMnPO_4$ at room temperature and at 50 °C. Fe-Mg co-substituted sample presents a very flat redox potential at ~4.1 V and a short potential at ~3.6 V versus Li/Li^+, respectively, corresponding to the phase transition process of $LiMnPO_4/MnPO_4$ and $LiFePO_4/FePO_4$. An increase of the redox potential from 3.45 to ~3.6 V in Fe^{2+}/Fe^{3+} is related to the lattice parameters and M-O (M = Mn, Mg and Fe) bond lengths [45]. The polarization decreased obviously as the test temperature increased, indicating an enhancement of electrochemical activity on unsubstituted and Fe-Mg co-substituted $LiMnPO_4$. This is proved by the electrochemical impedance spectra in Figure 3c. Although high discharged capacities were obtained at elevated temperature, low columbic efficiency was also found from Figure 3a. Even the charge specific capacity is higher than the theoretical specific capacity of 171 mAh g^{-1} for the Fe-Mg co-substituted sample tested at 50 °C. Similar behavior was reported by the other groups [26,46], ascribed to the side reactions or the passivation phenomena on electrode surface.

Figure 3b shows the cycling performance of unsubstituted and Fe-Mg co-substituted $LiMnPO_4$ at 0.1 C. The two samples delivered higher capacity when the working temperature increased from room temperature to 50 °C. The initial discharge capacity increased from 83.4 to 113.7 mAh g^{-1} for $LiMnPO_4$/C, which remained the capacity after 50 cycles at room temperature but not at 50 °C where the capacity faded rapidly to only 51% of the initial capacity. The capacity loss of $LiMnPO_4$/C was attributed to Jahn-Teller effect caused by Mn^{3+} and Mn dissolution in the electrolyte which is more serious at elevated temperature [6,19]. However, Fe-Mg co-substituted sample remains high discharge capacity and good cycling performance whether at room temperature or at elevated temperature. The discharge capacity of $LiMn_{0.9}Fe_{0.09}Mg_{0.01}PO_4$/C was above 150 mAh g^{-1} after 50 full charge/discharge cycles at 50 °C and the capacity loss was less than 5%.

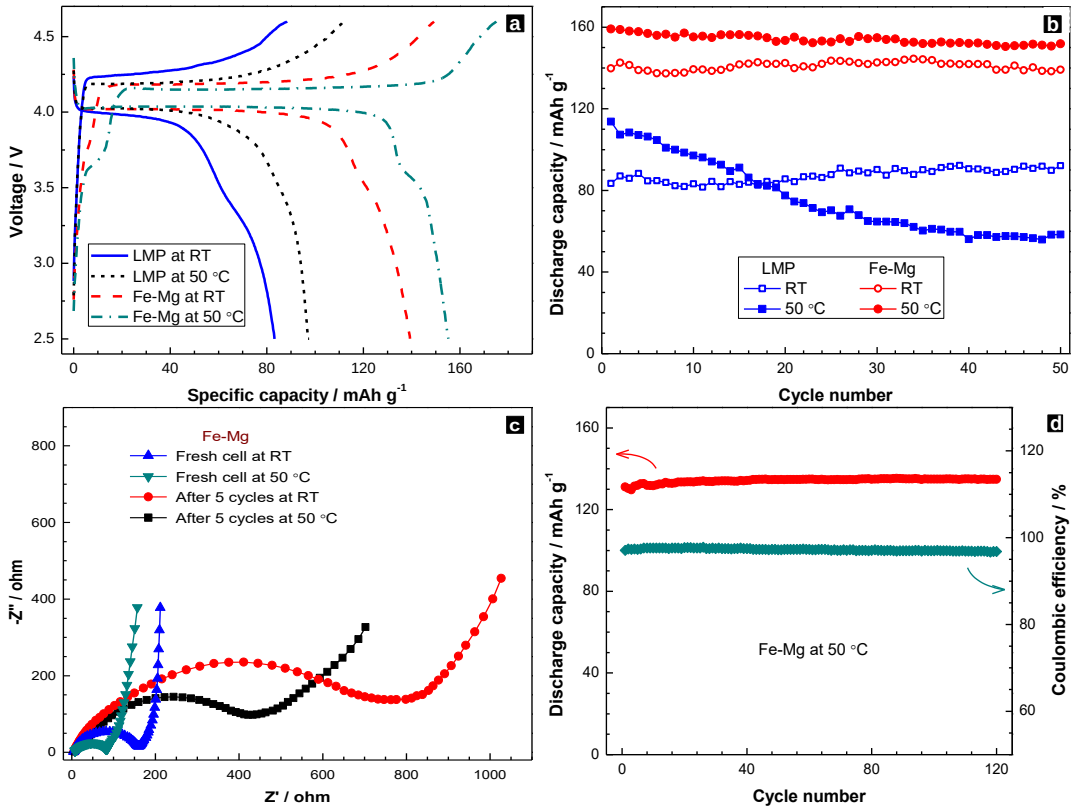

Figure 3. (a) Charge/discharge curves and (b) cycling performance of $LiMnPO_4$/C (LMP) and $LiMn_{0.9}Fe_{0.09}Mg_{0.01}PO_4$/C (Fe-Mg) at 0.1 C; (c) Nyquist plots of Fe-Mg sample using fresh cells and the cells after 5 full charge and discharge cycles and (d) cycling performance of Fe-Mg sample at 1 C.

The inductive effect leads to the strengthening of Mn-O bond and Mn ion is bound to the crystal lattice restraining the corrosion and dissolution of electrodes in electrolyte. In order to confirm the Mn dissolution in electrolyte, the half cells finished 50 cycles at 50 °C were disassembled and soaked in acetone for 24 h to detect the content of Mn using ICP. The concentrations of Mn dissolved in electrolyte are 83.6 ppm and 17.4 ppm for $LiMnPO_4$/C and $LiMn_{0.9}Fe_{0.09}Mg_{0.01}PO_4$/C respectively. It is obvious that Fe-Mg co-substitution reduces the Mn dissolution at elevated temperature and hence

significantly enhances the cycling performance of $LiMnPO_4$. Additionally, the introduction of Fe and Mg ion dilutes the Jahn-Teller distortion of Mn^{3+} [47] and electrochemical inactivity of Mg^{2+} remains unchanged during Li^+ insertion/extraction process that makes olivine structure more stable. Comparing with the results in recent reports from Table 1, the capacity loss of $LiMnPO_4$ materials at elevated temperature is decrease with the increase of Fe contents and coating carbon. Howerver, high Fe-contents or carbon-contents in $LiMnPO_4$ will lead to a decrease of energy density. In this work, only 10% Mn was substituted and the sample of $LiMn_{0.9}Fe_{0.09}Mg_{0.01}PO_4/C$ also exhibited excellent high rate performance at elevated temperature in Figure 3d. In the high charge and discharge rate of 1 C, it ketp the capacity of ~135 mAh g^{-1} during 120 cycles without capacity fade.

Table 1. Capacity loss of $LiMnPO_4$ at elevated temperature in recent reports

Sample	Discharge capacity at 1 C rate	Cycling conditions	Cycles	Capacity Loss ratio	Reference
$LiMn_{0.8}Fe_{0.2}PO_4$	155 mAh g^{-1}	2.0~4.5 V (CC-CV) at 50 °C	50	10%	[19]
$LiMn_{0.8}Fe_{0.2}PO_4/C$	160 mAh g^{-1}	2.0~4.5 V (CC-CV) at 50 °C	50	~4%	[19]
3DM-flakes $LiMnPO_4$	160 mAh g^{-1}	2.0~4.6 V (CC-CV) at 60 °C	40	~10%	[35]
$LiMn_{0.8}Fe_{0.2}PO_4/C$	/	2.2~4.5 V (CC-CV) at 45 °C	100	10%	[36]
$LiMn_{0.8}Fe_{0.2}PO_4/C$	154 mAh g^{-1}	2.0~4.5 V (CC-CV) at 55 °C	50	42%	[37]
CG-$LiMn_{0.8}Fe_{0.2}PO_4/C$	157 mAh g^{-1}	2.0~4.5 V (CC-CV) at 55 °C	50	~4%	[37]
$LiMn_{0.78}Fe_{0.2}Mg_{0.02}PO_4/C$	149 mAh g^{-1}	2.0~4.5 V (CC-CV) at 55 °C	100	16.4%	[38]
$LiMn_{0.48}Fe_{0.5}Mg_{0.02}PO_4/C$	161 mAh g^{-1}	2.0~4.5 V (CC-CV) at 55 °C	100	2.3%	[38]
C-$LiMnPO_4$/Graphene	104 mAh g^{-1}	2.5~4.5 V (CC-CV) at 55 °C	250	7%	[39]
$LiMn_{0.9}Fe_{0.09}Mg_{0.01}PO_4/C$	135 mAh g^{-1}	2.5~4.6 V (CC) at 50 °C	120	< 1%	This work

The above results suggest that Fe-Mg co-substitution improved the cycling stability of $LiMnPO_4$ even at elevated temperature. The inductive effect leads to the strengthening of Mn-O bond and Mn ion is bound to the crystal lattice restraining the corrosion and dissolution of electrodes in electrolyte. Additionally, the introduction of Fe and Mg ion dilutes the Jahn-Teller distortion of Mn^{3+} [47] and electrochemical inactivity of Mg^{2+} remains unchanged during Li^+ insertion/extraction process that makes olivine structure more stable.

4. CONCLUSIONS

The cycling stability of $LiMnPO_4$ at elevated temperature is Enhanced by Fe-Mg co-substitution. Fe-Mg co-substituted $LiMnPO_4$ generates M-O-P (M = Mn, Fe and Mg) inductive effect leading to the strengthening of Mn-O bond. It is restrained the Mn dissolutione in electrolyte by ICP analysis. Charge/discharge and cyclic voltammetry tests prove that Fe-Mg co-substitution improves the cycling stability of $LiMnPO_4$ at elevated temperature. No capacity loss is found after 120 cycles for $LiMn_{0.9}Fe_{0.09}Mg_{0.01}PO_4/C$ tested at 50 °C. This paves a way to make $LiMnPO_4$ towards to practical

application.

ACKNOWLEDGEMENTS
Financial support from Hubei Provincial Natural Science Foundation of China (2015CFA146 and 2013CFC100), Hubei Provincial Department of Education (B2014040) and Hubei Polytechnic University (14cx13, 13xjz03R and 13xtz09) is gratefully acknowledged.

References

1. A.K. Padhi, K.S. Nanjundaswamy, J.B. Goodenough, *J. Electrochem. Soc.*, 144 (1997) 1188.
2. L. Wang, X. He, W. Sun, J. Wang, Y. Li, S. Fan, *Nano Lett.*, 12 (2012) 5632.
3. X. Huang, X. He, C. Jiang, G. Tian, Y. Liu, *Ind. Eng. Chem. Res.*, 56 (2017) 10648.
4. C. Huang, D. Ai, L. Wang, X. He, *Chem. Lett.*, 42 (2013) 1191.
5. C. Masquelier, L. Croguennec, *Chem. Rev.*, 113 (2013) 6552.
6. V. Aravindan, J. Gnanaraj, Y. Lee, S. Madhavi, *J. Mater. Chem. A*, 1 (2013) 3518.
7. S. Wi, J. Park, S. Lee, J. Kang, T. Hwang, K. Lee, H. Lee, S. Nam, C. Kim, Y. Sung, B. Park, *Nano Energy*, 31 (2017) 495.
8. B. Kang, G. Ceder, *J. Electrochem. Soc.*, 157 (2010) A808.
9. Y. Sun, S. Oh, H. Park, B. Scrosati, *Adv. Mater.*, 23 (2011) 5050.
10. L. Wang, L. Zhang, J. Li, J. Gao, C. Jiang, X. He, *Int. J. Electrochem. Sc.*, 7 (2012) 3362.
11. Z. Dai, L. Wang, F. Ye, C. Huang, J. Wang, X. Huang, J. Wang, G. Tian, X. He, M. Ouyang, *Electrochim. Acta*, 134 (2014) 13.
12. C. Xu, L. Wang, X. He, J. Luo, Y. Shang, J. Wang, *Int. J. Electrochem. Sc.*, 11 (2016) 1558.
13. X. Cao, A. Pan, Y. Zhang, J. Li, Z. Luo, X. Yang, S. Liang, G. Cao, *Acs Appl. Mater. Inter.*, 8 (2016) 27632.
14. M. Yonemura, A. Yamada, Y. Takei, N. Sonoyama, R. Kanno, *J. Electrochem. Soc.*, 151 (2004) A1352.
15. J. Moskon, M. Pivko, I. Jerman, E. Tchernychova, N.Z. Logar, M. Zorko, V.S. Selih, R. Dominko, M. Gaberscek, *J. Power Sources*, 303 (2016) 97.
16. Y. Xie, H. Yu, T. Yi, Y. Zhu, *Acs Appl. Mater. Inter.*, 6 (2014) 4033.
17. Z.X. Nie, C.Y. Ouyang, J.Z. Chen, Z.Y. Zhong, Y.L. Du, D.S. Liu, S.Q. Shi, M.S. Lei, *Solid State Commun.*, 150 (2010) 40.
18. A. Yamada, M. Hosoya, S. Chung, Y. Kudo, K. Hinokuma, K. Liu, Y. Nishi, *J. Power Sources*, 119 (2003) 232.
19. L. Yang, Y. Xia, X. Fan, L. Qin, B. Qiu, Z. Liu, *Electrochim. Acta*, 191 (2016) 200.
20. S.M. Oh, S.W. Oh, C.S. Yoon, B. Scrosati, K. Amine, Y.K. Sun, *Adv. Funct. Mater.*, 20 (2010) 3260.
21. S.K. Martha, B. Markovsky, J. Grinblat, Y. Gofer, O. Haik, E. Zinigrad, D. Aurbach, T. Drezen, D. Wang, G. Deghenghi, I. Exnar, *J. Electrochem. Soc.*, 156 (2009) A541.
22. K. Rajammal, D. Sivakumar, N. Duraisamy, K. Ramesh, S. Ramesh, *Ionics*, 22 (2016) 1551.
23. T. Drezen, N. Kwon, P. Bowen, I. Teerlinck, M. Isono, I. Exnar, *J. Power Sources*, 174 (2007) 949.
24. H. Dinh, S. Mho, Y. Kang, I. Yeo, *J. Power Sources*, 244 (2013) 189.
25. B. Zou, R. Yu, M. Deng, Y. Zhou, J. Liao, C. Chen, *Rsc Adv.*, 6 (2016) 52271.
26. D. Choi, D. Wang, I. Bae, J. Xiao, Z. Nie, W. Wang, V.V. Viswanathan, Y.J. Lee, J. Zhang, G.L. Graff, Z. Yang, J. Liu, *Nano Lett.*, 10 (2010) 2799.
27. L. Wang, P. Zuo, G. Yin, Y. Ma, X. Cheng, C. Du, Y. Gao, *J. Mater. Chem. A*, 3 (2015) 1569.
28. S.K. Martha, J. Grinblat, O. Haik, E. Zinigrad, T. Drezen, J.H. Miners, I. Exnar, A. Kay, B. Markovsky, D. Aurbach, *Angew. Chem. Int . Ed.*, 48 (2009) 8559.

29. H. Fang, H. Yi, C. Hu, B. Yang, Y. Yao, W. Ma, Y. Dai, *Electrochim. Acta*, 71 (2012) 266.
30. D. Wang, C. Ouyang, T. Drézen, I. Exnar, A. Kay, N. Kwon, P. Gouerec, J.H. Miners, M.K. Wang, M. Grätzel, *J. Electrochem. Soc.*, 157 (2010) A225.
31. J. Zhang, S. Luo, L. Chang, A. Hao, Z. Wang, Y. Liu, Q. Xu, Q. Wang, Y. Zhang, *Appl. Surf. Sci.*, 394 (2017) 190.
32. Q. Huang, Z. Wu, J. Su, Y. Long, X. Lv, Y. Wen, *Ceram. Int.*, 42 (2016) 11348.
33. C. Hu, H. Yi, H. Fang, B. Yang, Y. Yao, W. Ma, Y. Dai, *Electrochem. Commun.*, 12 (2010) 1784.
34. P.R. Kumar, M. Venkateswarlu, M. Misra, A.K. Mohanty, N. Satyanarayana, *J. Electrochem. Soc.*, 158 (2011) A227.
35. H. Yoo, M. Jo, B. Jin, H. Kim, J. Cho, *Adv. Energy Mater.*, 1 (2011) 347.
36. H. Xu, J. Zong, F. Ding, Z. Lu, W. Li, X. Liu, *Rsc Adv.*, 6 (2016) 27164.
37. L. Yang, Y. Xia, L. Qin, G. Yuan, B. Qiu, J. Shi, Z. Liu, *J. Power Sources*, 304 (2016) 293.
38. B. Zou, Y. Shao, Z. Qiang, J. Liao, Z. Tang, C. Chen, *J. Power Sources*, 336 (2016) 231.
39. X. Fu, K. Chang, B. Li, H. Tang, E. Shangguan, Z. Chang, *Electrochim. Acta*, 225 (2017) 272.
40. D. Di Lecce, T. Hu, J. Hassoun, *J. Alloy. Compd.*, 693 (2017) 730.
41. F. Cheng, J. Liang, Z. Tao, J. Chen, *Adv. Mater.*, 15 (2011) 695.
42. B.L. Ellis, K.T. Lee, L.F. Nazar, *Chem. Mater.*, 22 (2010) 691.
43. H. Yi, C. Hu, H. Fang, B. Yang, Y. Yao, W. Ma, Y. Dai, *Electrochim. Acta*, 56 (2011) 4052.
44. R.D. Shannon, *Acta Cryst.*, 32 (1976) 751.
45. T. Muraliganth, A. Manthiram, *J. Phys. Chem. C*, 114 (2010) 15530.
46. T.N.L. Doan, Z. Bakenov, I. Taniguchi, *Adv. Powder Technol.*, 21 (2010) 187.
47. G. Chen, A.K. Shukla, X. Song, T.J. Richardson, *J. Mater. Chem.*, 21 (2011) 10126.